



Article

Microbial Population Dynamics and the Role of Sulfate Reducing Bacteria Genes in Stabilizing Pb, Zn, and Cd in the Terrestrial Subsurface

Ranju R. Karna ^{1,2,*}, Ganga M. Hettiarachchi ¹, Joy Van Nostrand ³ , Tong Yuan ³, Charles W. Rice ⁴, Yared Assefa ¹ and Jizhong Zhou ^{3,5,6}

¹ Soil and Environmental Chemistry Laboratory, Department of Agronomy, Kansas State University, Manhattan, KS 66506, USA; ganga@ksu.edu (G.M.H.); yareda@ksu.edu (Y.A.)

² Oak Ridge Institute for Science and Education, Oak Ridge, TN 37830, USA

³ Institute of Environmental Genomics and Department of Microbiology and Plant Biology, University of Oklahoma, Norman, OK 73019, USA; joy.vannostrand@ou.edu (J.V.N.); 15838348600@163.com (T.Y.); jzhou@rccc.ou.edu (J.Z.)

⁴ Soil Microbial Ecology Laboratory, Department of Agronomy, Kansas State University, Manhattan, KS 66506, USA; cwrice@ksu.edu

⁵ Earth Sciences Division, Lawrence Berkeley National Laboratory, Berkeley, CA 94720, USA

⁶ School of Environment, Tsinghua University, Beijing 100084, China

* Correspondence: karna.ranju@epa.gov; Tel.: +1-513-487-2449

Received: 20 August 2018; Accepted: 31 October 2018; Published: 3 November 2018



Abstract: Milling and mining metal ores are major sources of toxic metals contamination. The Spring River and its tributaries in southeast Kansas are contaminated with Pb, Zn, and Cd because of 120 years of mining activities. Trace metal transformations and cycling in mine waste materials greatly influence their mobility and toxicity and they affect both plant productivity and human health. It has been hypothesized that under reduced conditions in sulfate-rich environments, these metals can be transformed into their sulfide forms, thus limiting mobility and toxicity. We studied biogeochemical transformations of Pb, Zn, and Cd in flooded subsurface mine waste materials, natural or treated with organic carbon (OC), and/or sulfur (S), by combining advanced microbiological and X-ray spectroscopic techniques to determine the effects of treatments on the microbial community structure and identify the dominant functional genes that are involved in the biogeochemical transformations, especially metal sulfide formation over time. Samples collected from medium-, and long-term submerged columns were used for microarray analysis via functional gene array (GeoChip 4.2). The total number of detected gene abundance decreased under long-term submergence, but major functional genes abundance was enhanced with OC-plus-S treatment. The microbial community exhibited a substantial change in structure in response to OC and S addition. Sulfate-reducing bacteria genes *dsrA/B* were identified as key players in metal sulfide formation via dissimilatory sulfate reduction. Uniqueness of this study is that microbial analyses presented here in detail are in agreement with molecular-scale synchrotron-based X-ray data, supporting that OC-plus-S treatment would be a promising strategy for reducing metal toxicity in mine waste materials in the subsurface environment.

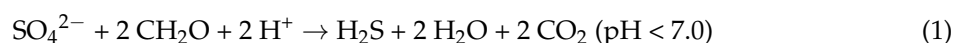
Keywords: mine waste; lead; zinc; cadmium; sulfate-reducing bacteria; biogeochemical processes

1. Introduction

Generation of large amounts of mine waste containing several toxic metals is the main environmental concern associated with milling and mining activities [1,2]. Toxic metals are transported

via different pathways such as wind erosion and surface water runoff to neighboring water bodies [3,4]. The Tri-State mining district in parts of southeast Kansas, southwest Missouri, and northeast Oklahoma was one of the largest Pb and Zn ore-mining districts in the world for 120 years (until 1970). The movement of soluble metals and metal-laden sediments from the landscape into surface waters via surface runoff are the primary ecological concerns for both aquatic and terrestrial organisms [5]. The US Environmental Protection Agency (US EPA) has suggested wetland construction as a remediation strategy for soils that are highly contaminated by abandoned mine waste materials with the hypothesis that these metals could be transformed into their sulfide forms under reduced conditions in sulfate-rich environments, thus limiting their mobility and toxicity.

Several main challenges are associated with this strategy. Mine waste material with low dissolved OC content could have significant effects on redox processes [6–8], because OC is the main driver of biogeochemical cycling of major and trace elements [9,10]. Additionally, limited S in mine waste could limit sulfide formation and promote carbonate precipitation, depending on pH and carbonate concentration [11]. Therefore, the addition of OC and S could facilitate these metals to be transformed back into their sulfide forms under reduced conditions, thereby limiting their mobility and toxicity. According to Stein [7], a generalized sulfate reduction reaction using organic matter (OM) as an electron donor is:



At high metal concentrations, metals tend to precipitate as metal sulfides around circumneutral pH, because the rate of H₂S formation increases at a pH of 7.0 to a maximum of 8.0 [12,13]:



The above-mentioned reaction is the result of dissimilatory sulfate metabolism that has been tested and successfully removed contaminants via biostimulation. Of all the metal sulfide minerals, iron sulfide mineralization is most often attributed to microbial activity [14], especially to the activity of dissimilatory sulfate-reducing bacteria (SRB). Environmentally important activities that are displayed by SRB are the result of metabolic production of high levels of sulfide that are reactive and participate in subsequent mineral formation [14,15].

Using a culture-dependent technique would not be feasible to study the complex microbial community because 99% of microorganisms have not been cultured [16]; therefore, culture-independent techniques, such as functional gene arrays (FGA), are required [17,18]. GeoChip 4.2 is a functional gene array that contains 83,992 oligonucleotides (50-mer) probes targeting 152,414 genes in 410 gene categories from more than 5200 microbial strains including bacteria, archaea, fungi, and viruses. These genes are involved in the biogeochemical processes and functional activities of microbial communities important to human health, ecosystem management, agriculture, energy, global climate change, and environmental cleanup and restoration, including N, C, S, and P cycling, metal reduction and resistance, and organic contaminant degradation [19]. This technique enables detection, characterization, and quantification of microorganisms in mine waste and links microbial diversity to ecosystem processes and functions [17,20]. The approach has been used successfully to track the dynamics of metal-reducing bacteria and associated communities for an in situ bioremediation study [18,20,21].

Phospholipid fatty acid analysis (PLFA) is another rapid, inexpensive, and efficient way to determine the effect of treatments on microbial community structures [22]. Certain PLFAs markers can serve as unique signatures for a group. However, such biomarkers cannot detect individual microbial species due to overlapping PLFA patterns; nevertheless, a whole PLFA pattern is used to elucidate the shift in community composition and their relation to specific metabolic and environmental conditions [23].

Few studies have combined microbial analysis with solution chemistry and microscopic and X-ray spectroscopic techniques to develop a complete molecular-scale understanding of complex

biogeochemical processes affecting soil and water [24,25]. This study attempted to explore the interplay between geochemical and biological processes in the transformation of Pb, Zn, and Cd in natural subsurface environments biostimulated by the addition of OC and S. Stimulating the systems with OC and S would favor SRB growth and activities. We expect that OC-plus-S treatment would result in a higher abundance of SRB genes as compared with natural, OC alone, or S alone treatments. Study objectives were to: (a) characterize the microbial community playing a role in the biogeochemical transformation of Pb, Zn, and Cd under reduced conditions, (b) measure the change in microbial community structure with OC and/or S treatment over medium- and long-term incubation, and (c) identify the most dominant genes and associated mechanisms that are involved in effective immobilization of Pb, Zn, and Cd.

2. Materials and Methods

2.1. Sample Collection and Characterization

Contaminated mine waste materials were collected from a secured repository area in Baxter Springs, KS, a part of the Tri-State mining district that has a 120-year history of Pb- and Zn-ore mining related activities. The mine waste materials were sieved to 2-mm size. The pH of a water extract (water: mine waste ratio of 2:1) was determined using Orion Ag/AgCl pH electrode. Particle size distribution was determined using a modification of the pipet method of Kilmer et al. [26], and method 3A1 from the Soil Survey Laboratory Method Manual [27]. The sieved materials were digested using the aqua-regia reflux solid digestion method [28]. The digested samples were analyzed on inductively coupled plasma- optical emission spectroscopy (ICP-OES) to determine the total dissolved element concentrations for Pb, Zn, Cd, Fe, S, Mn, and other transition metal elements. In addition, total N and C content was measured using LECO TruSpec CN Carbon/Nitrogen combustion analyzer (LECO Corporation, St. Joseph, MI, USA).

2.2. Treatment Application and Experimental Setup

For S-treatment application, sodium sulfate (Na_2SO_4) solution was added to the mine waste material to provide S at a ratio of 1:2 mM of sum of metals present in material: mM of S. The metal concentrations used for the summation were Pb, Zn, Cd, Fe, and Mn. The treated materials were equilibrated for 10 days at room temperature on a reciprocating shaker (6010, Eberbach Corporation, Ann Arbor, MI, USA) at 192 reciprocates/min for three days, and at 92 reciprocates/min for the remaining seven days. After equilibration, S-treated mine waste was leached with deionized (DI) water to reduce salinity until a target electrical conductivity of $<2 \text{ mS cm}^{-1}$ was achieved, then the material was air-dried. All the treated and untreated mine waste materials were inoculated with 0.5 g (per 100 g of material) of soil slurry (Ivan, Kennebec, and Kahola silt loams) collected from the North Agronomy Farm at Kansas State University, Manhattan, KS. The serial dilution of soil slurry was cultured on a Petri dish using Postgate's medium and incubated overnight at 34°C in an anaerobic jar (AG0025A used with oxygen absorber; OXAN0025A, Fisher Scientific, Pittsburgh, PA, USA). The black patches observed on the plate indirectly confirmed the presence of SRB in the soil slurry. The method used for SRB culturing was adapted from Luptakova et al. [29]. The mine waste materials (non-treated or treated with S) were well mixed with soil slurry and used to pack Plexiglas columns (20 cm length, 3.2 cm ID with three windows milled at 2.8 cm, 9.84 cm, and 16.94 cm along the column length) to achieve a bulk density of about 1.7 g cm^{-3} . The packed columns were saturated slowly with DI water using a Mariotte's bottle that delivered a constant flow rate before the eluent solution was supplied. The eluent consisted of a base of simulated groundwater (1 mM NaCl, 1 mM MgCl_2 , 1 mM KCl, 1 mM CaCl_2 adjusted to pH 7.2) with or without 10.7 mM Na-lactate (32 mM OC). This eluent provided four treatments for the columns designated as C0S0, C1S0, C0S1, and C1S1, where C0 and C1 indicate columns where the added simulated groundwater was without OC or with OC, respectively, and S0 and S1 indicate columns where the added simulated groundwater

was without additional S or with additional S, respectively. Each treatment combination had two replicates due to limited space being available in the glovebox. The eluent solution was supplied using a syringe pump (KD Scientific Inc., Holliston, MA, USA) at the rate of 13 mm day⁻¹ to simulate a slow groundwater discharge rate [30]. Three series of column experiments, short (32-day), medium (119-day), and long-term (252-day), were conducted at room temperature ~25 °C at different times due to the lack of space in the anaerobic chamber to conduct them all simultaneously. All three series of experiments were conducted based on a completely randomized design with a two-way factorial experiment (factor 1: OC with two levels, 0 and 10.7 mM L⁻¹; factor 2: S with two levels, 0 and 252.7 mg kg⁻¹). However, the short-term experiment was utilized only as a preliminary experiment. Effluent samples were collected weekly for medium-term and biweekly for long-term submergence, and they were analyzed for pH, redox potential, total dissolved elements (for Pb, Cd, Zn, Fe, S, Mn, K, Ca, Mg, Na), anions (for sulfate, nitrate, nitrite, chloride, phosphate), and dissolved organic carbon (DOC) measurements. At the end of each column experiment, about 20-g mine waste samples were collected at the 1.2- to 3.2-cm depth from the port located at the height of 18 cm (far end) from all columns and frozen at -80 °C for DNA extraction and X-ray absorption spectroscopy (XAS). More details on solution chemistry data collection, approaches used in synchrotron-based X-ray analysis, and their outcomes can be found in Karna et al. [31].

2.3. Phospholipid Fatty Acid (PLFA) Analysis

The PLFA analysis was performed as an initial measurement to determine the microbial community changes with OC and S treatment prior to microarray analysis. For this, PLFA extraction was done on the original mine waste materials, and submerged C0S0 and C1S1 treatments from medium-term study only due to the lack of samples from other treatments. The extraction was based on single phase extraction of lipids, which was then methylated to give fatty acids methyl esters (FAME) and then analyzed by gas chromatograph.

The PLFA extraction was performed by following the method of Bligh and Dyer [32], as modified by White and Ringberg [33]. The resulting FAME were analyzed using a Thermo Scientific Trace GC-ISQ mass spectrometer (Thermo Scientific, Germany) with helium as a carrier gas. Analysis was conducted in the electron impact (70 eV) mode. Peaks were identified based on retention times of commercially available bacterial acid methyl esters (BAME; Matreya 1114) standard mix. The methyl ester peaks that were not present in the BAME mix were tentatively assigned through mass spectral interpretation by comparison with spectra from a library (Wiley 138K mass spectral database). An internal standard, nonadecanoic acid methyl ester (19:0), was used to quantify the sample peaks based on the comparative abundance (nmol g⁻¹). Fatty acids were grouped based on criteria that were provided by McKinley et al. [34], whereby Gram-positive bacteria were branched monounsaturated cyclopropane (i-15:0, a-15:0, i-16:0, i-17:0, and a-17:0). Gram-negative biomarkers are cyclopropane PLFAs (2-OH 12:0, 3-OH 12:0, 2-OH 14:0, 3-OH 14:0, 2-OH 16:0, C16_1_9_cis, C16_0_2-OH, 16:1 ω 7c, 18:1 ω 7c, cy17:0, cy19:0), while actinomycetes is 10Me18:0. Fungi biomarkers are polyunsaturated PLFAs (18:1 ω 5c, 18:2 ω 9, 12C, 18:2 ω 6,9,12), while arbuscular mycorrhizae fungi (AMF) is 16:1 ω 5c, and *Desulfovibrio* biomarker is i_17_1 [34].

2.4. GeoChip Analysis

Microarray analysis was performed on all the treatment combinations, C0S0, C0S1, C1S0, and C1S1, from medium-term study, whereas only C0S0 and C1S1 treatment combinations were used from long-term study. The samples selection for the long-term study was done based on the geochemical and spectroscopic results that were obtained from medium-term study. There were only two replicate columns per treatment. Rather than doing two technical replicates for each sample, we pooled the two biological replicates to create one technical replicate. Pooled samples average out technical variation.

2.5. DNA Extraction, Labeling, Hybridization, Scanning, and Data Processing

About 5 g of soil was used for genomic DNA extraction using the PowerMax soil DNA isolation kit (Mo Bio, Carlsbad, CA, USA). Raw DNA extracts were purified using Wizard Plus SV Minipreps purification system (Promega Biosciences, San Luis Obispo, CA, USA). Purified DNA was quantified using the Quant-iT PicoGreen dsDNA assay kit (Promega Biosciences, San Luis Obispo, CA, USA). DNA was labeled then hybridized at 42 °C on GeoChip 4.2, as described in Lu et al. [21]. After hybridization, arrays were scanned with a NimbleGen MS 200 Microarray Scanner, and then Nimble Scan software (Roche NimbleGen, Madison, WI, USA) was used for data extraction and quantification. Data preprocessing and normalization using common oligonucleotide reference standards [35] was performed as described by Lu et al. [21].

Statistical analyses were performed using SAS for Windows version 9.2 (SAS Institute Inc., Cary, NC, USA). The data were analyzed using PROC ANOVA. Tukey's Honestly Significant Difference (HSD) test was used for means separation ($\alpha = 0.05$). Dissimilarity test was also conducted by using the software that is available at the Institute of Environmental Genomics (IEG) website, OU, OK (Table S3). All hybridization data are available at <http://www.agronomy.k-state.edu/research/soil-and-environment/soil-environment-chem/Research%20Data.html>.

3. Results

3.1. General Characterization of Mine Waste Materials

The mine waste material consisted of 85% sand (2000 to 50 μm), 11.3% silt (50 to 2 μm), and 3.4% clay (<2 μm). Total N and C were 0.03 g kg⁻¹ and 1.56 g kg⁻¹, respectively. The pH of the water extract (DI water: geomaterial mass ratio, 2:1) was 7.2, and the electrical conductivity was 2.31 mS cm⁻¹. Selected total elemental concentrations of Pb, Zn, and Cd in the material were 5048, 23,468, and 67 mg kg⁻¹, respectively (Table S1). The standard reference material 2711a (National Institute of Standards and Technology, Gaithersburg, MD) was digested along with the geomaterial to ensure a recovery percentage of each element that ranged from 79 to 109%.

3.2. Preliminary Microbial Community Characterization

The PLFA analysis results on starting original mine tailings, inoculum, non-amended control, and amended materials submerged for 119 days indicated the presence of biomarkers for various microbial groups (Gram-, Gram+, AMF, fungi, *Desulfovibrio*, and Actinomycetes). Total PLFA in starting mine waste materials was 2.42 nmolg⁻¹, whereas it was 6.18 nmolg⁻¹ in the submerged sediment that was used as inoculum (Table S2). Once the materials were inoculated and submerged, no significant difference in summed abundance of PLFA biomarkers ($\rho = 0.33$), as well as other biomarkers (Gram- ($\rho = 0.29$), Gram+ ($\rho = 0.27$), AMF ($\rho = 0.29$), fungi ($\rho = 0.81$), *Desulfovibrio* ($\rho = 0.33$), and Actinomycetes ($\rho = 0.52$)) were measured in both non-amended and amended treatments at 119 days with comparison to the starting material (Table S2). The results from PLFA analysis falls in agreement with the microarray analysis results that indicated no significant difference in the total number of detected genes among the treatments at 119-day submergence.

3.3. X-ray Absorption Spectroscopy

Multiple synchrotron-based techniques have been used to enhance quantitative mineral species identification [36,37]. Micro-, and bulk-X-ray absorption spectroscopy (XAS), as well as micro-X-ray diffraction (μ -XRD) techniques were used to identify the minerals in the original mine waste material in this study. The results agree between μ -XRD and bulk XAS techniques and indicated presence of silicate, carbonate, sulfate, phosphate, nitrate, and oxide minerals (Figure 1), which are supported by other studies conducted on smelter-impacted soils [36–39]. Bulk-XAS speciation conducted for Pb, Zn, and Cd in the starting mine waste material used in this study indicated that there were no detectable levels of metal sulfides, but became more detectable under submerged conditions,

and enhanced due to amendments and time. About 62% galena (PbS), 31% sphalerite (ZnS), and 39% Cd-sulfide were detected in C1S1 when compared to none in C0S0 (Figure 1 in this manuscript) under long-term incubation. Instead, more carbonates were formed in non-amended (C0S0) flooded materials. Please see more details and published data in Karna et al. [31].

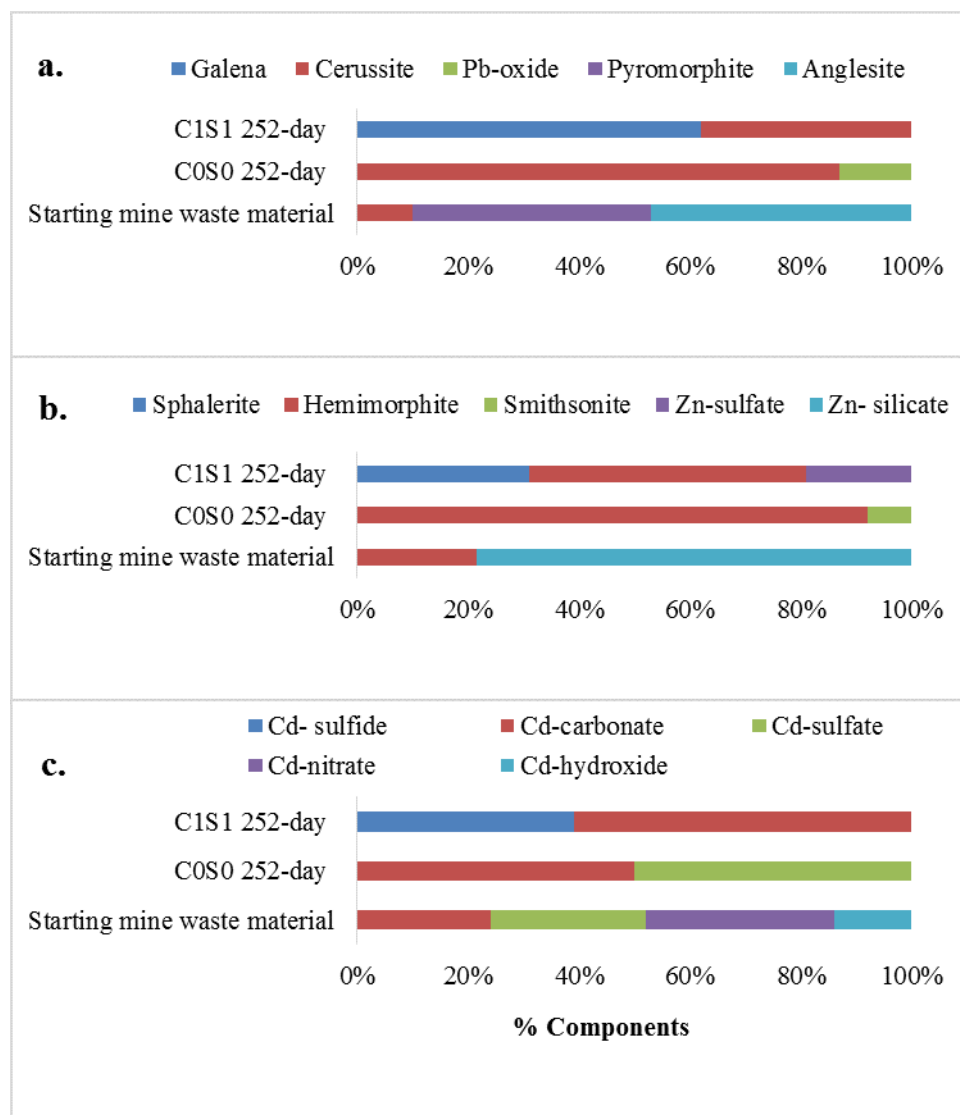


Figure 1. X-ray absorption fine structure spectroscopy results showing % components for (a) lead, (b) zinc, and (c) cadmium in starting mine waste material, control (C0S0), and OC-plus-S-treated sample (C1S1) under long-term (252-day) submergence. Phases identified as less than 10% may not be significant due to error that is associated with smaller estimations.

The total number of detected genes showed that functional gene richness in C1S1 was slightly enhanced but not statistically significant from any of the other treatments under medium-term submergence (Figure 2). In contrast, under long-term submergence, the total number of detected genes significantly decreased in both C0S0 and C1S1 treatments.

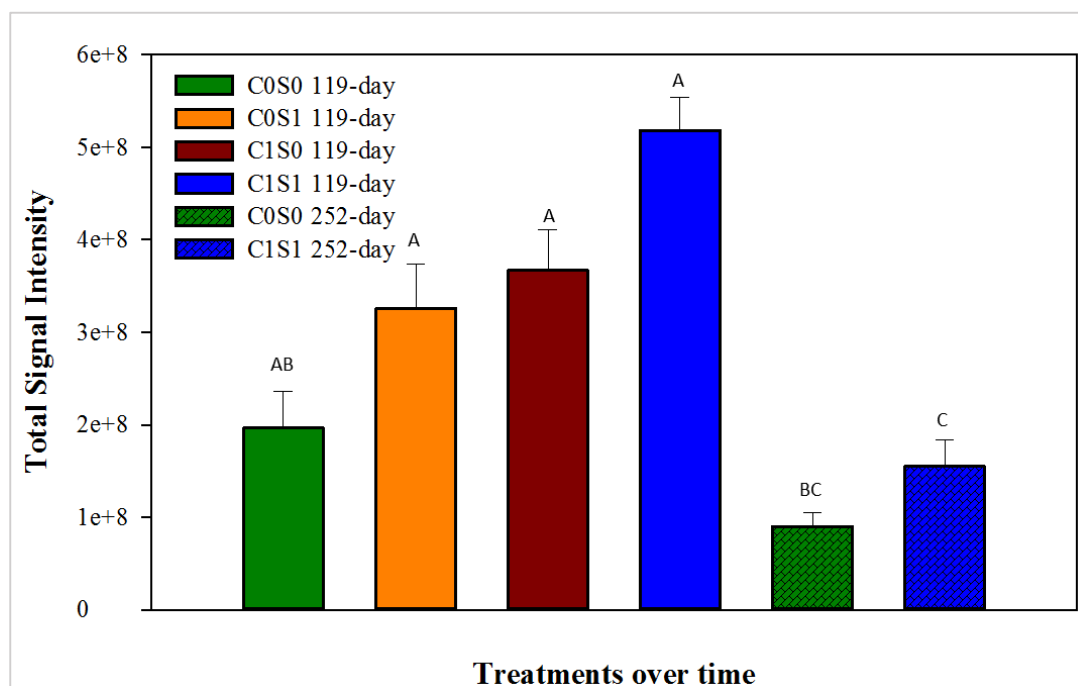


Figure 2. Functional gene richness under medium- (119-day) and long-term (252-day) submergence. All the treatments, C0S0, C0S1, C1S0, and C1S1 (solid filled bars), from medium-term submergence, and only C0S0 and C1S1 (pattern filled bars) from long-term submergence are plotted. Vertical bars represent the mean of three replicates; 2 biological replicates from the individual columns and 1 technical replicate pooled from each biological column. Bars with the same letters are not significantly different. Different letters within a category indicate significance difference ($\alpha = 0.05$).

3.4. Relationships among Microbial Communities

Detrended correspondence analysis (DCA) was used to examine the overall functional structure changes in microbial communities with the OC-plus-S treatment under medium- and long-term submergence. The ellipses were drawn to determine the clusters based on the observations. When samples from medium- and long-term submergence were plotted individually, separate clusters for each treatment were formed (Figure S1), indicating an overall effect of OC and/or S treatments and time on the community structure in relation to geochemistry dynamics and enhanced reduction (Figure 3). This change in clustering with longer submergence is not unusual, because time was such a strong driver in this system especially when both OC and S were applied. When all samples were analyzed together, 252-day samples were clearly separated from 119-day samples, suggesting that time was another strong driver in this system. Within the 252-day samples, two clusters were apparent—one for samples with added OC and S and then other for samples with no amendment. There is some separation in the 119-day samples with most of the OC amended samples at the top of the cluster and those with no OC amendment at the bottom. When the time variable was eliminated by removing 252-day samples, the effects of OC and S became more apparent. There is a clear separation of OC amended and unamended samples and some separation between the S amended and unamended samples, especially if OC was present as well.

Under 119 days submergence, the DCA ordination plot for C-cycling genes indicated clear cluster for C1S0 when only OC was added (Figure S3). Similarly, the DCA plots of the S-cycling category, and S-genes, such as *dsrA* and *dsrB*, segregated much clearly for C0S1 and C1S1 when S was added, and no overlapping was observed with respect to 119 days versus 252 days of submergence specifically for *dsrA* genes (Figures S4–S6). Under 252 days submergence, both treatments, C0S0 and C1S1 samples, made separate clusters under each category.

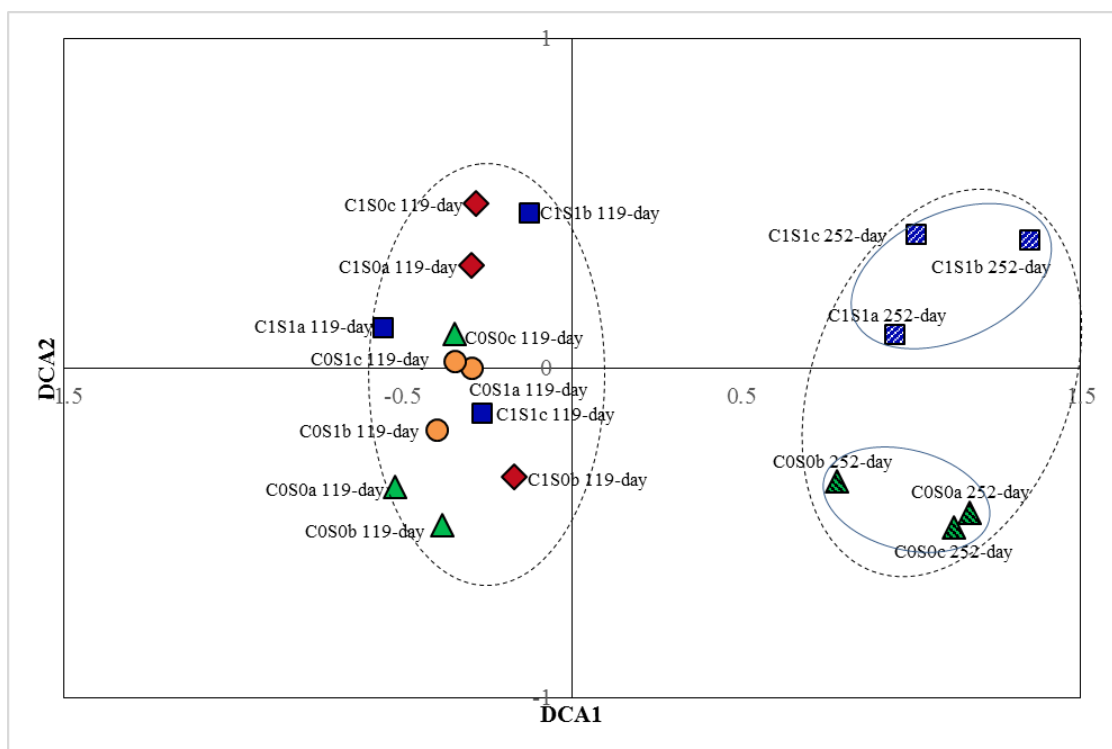


Figure 3. Detrended correspondence analysis (DCA) for the total number of detected genes under medium- (119-day) and long-term (252-day) submergence, indicating community structure changes. All the treatments, C0S0, C0S1, C1S0, and C1S1 (solid filled markers), from medium-term submergence, and only C0S0 and C1S1 (pattern filled markers) from long-term submergence are plotted.

3.5. Total Abundance of Functional Gene Categories

The shifts that were observed in the DCA ordination plots were likely the result of changes in total abundance of functional genes. The abundance of metal resistance and organic remediation genes were significantly enhanced in C1S1, even though the total number of detected genes decreased by 26% (Figure 4a) and 21% (Figure 4b), respectively, over 252 days of submergence. Sulfur- and C-cycling functional gene abundance was enhanced by 35% and 27%, respectively, in C1S1 in comparison with C0S0 at 252 days submergence (Figure 4a).

Thus, significant enrichment of S- ($\rho = 0.01$) and C-cycling genes ($\rho = 0.01$) and a large decrease in metal resistance ($\rho = 0.001$) and organic remediation genes by 50 to 60% ($\rho = 0.001$) within both treated and untreated samples at 252 days of submergence could have resulted in community structure changes. Functional genes involved in S- and C-cycling were significantly enhanced in C1S1, even though the total number of detected genes decreased under 252 days submergence, indicating the direct involvement of S- and C-cycling genes in biogeochemical transformation processes.

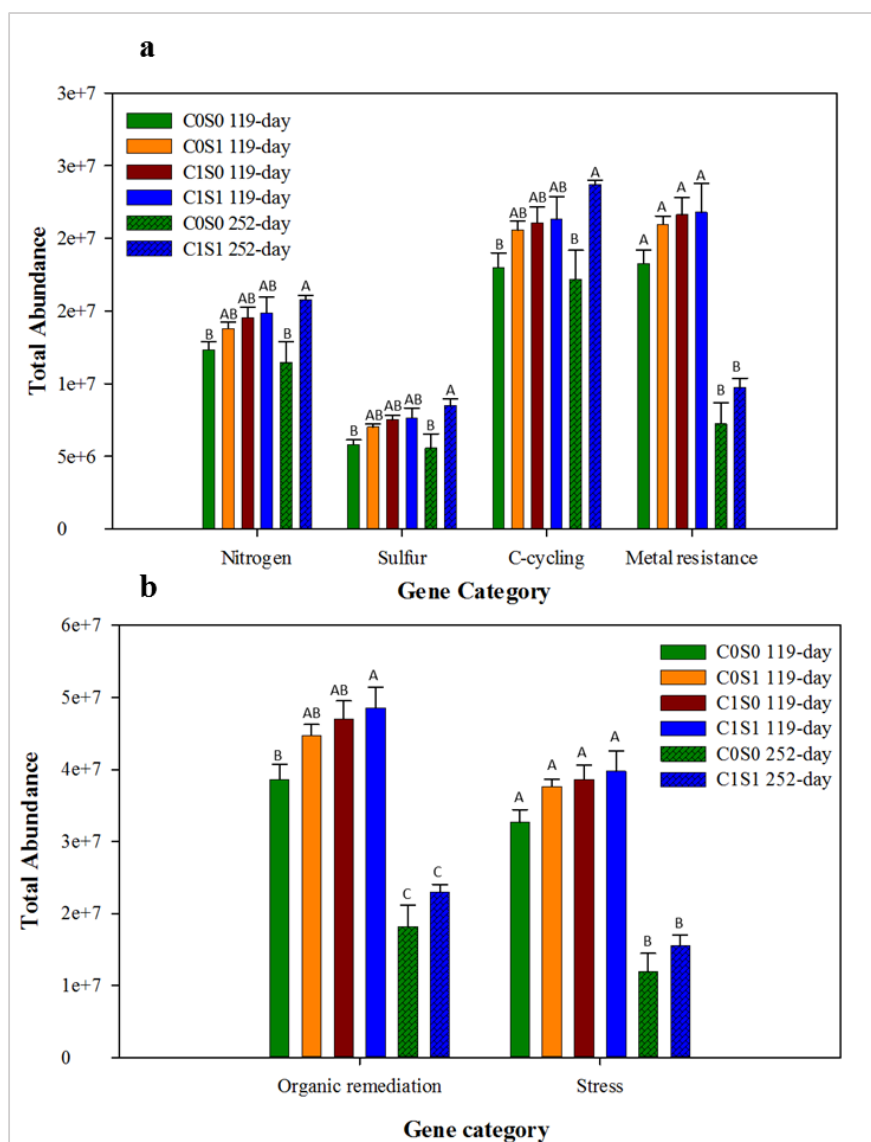


Figure 4. Total abundance of function genes in (a) nitrogen, sulfur, c-cycling and metal resistance categories, (b) organic remediation and stress categories for the samples submerged for both medium- (119-day) and long-term (252-day) submergence. All the treatments, C0S0, C0S1, C1S0, and C1S1 (solid filled bars), from medium-term submergence, and only C0S0 and C1S1 (pattern filled bars) from long-term submergence are plotted. Vertical bars represent the mean of three replicates; two biological replicates from the individual columns, and one technical replicate pooled from each biological column. Bars with the same letter are not significantly different. Different letters within a category indicate significance difference ($\alpha = 0.05$).

3.6. Changes in S-, C-Cycling, and Metal Resistance Genes

To better understand the differences observed in the categories above, changes in individual genes were examined. Sulfate-reducing bacteria mediate the direct and indirect reduction of heavy metals and metalloids [13,40] and they have been considered key players in anaerobic bioremediation for contaminated soils, waters, and subsurface [41,42]. In SRB, the *dsr* gene encodes the dissimilatory sulfite reductase enzyme with subunits, and A/B is a key enzyme in reducing sulfite to sulfide and is required by all sulfate reducers [43]. Thus, *dsr* genes provide insight into SRB activities and their functional role in sulfate reduction. Under S-cycling, *dsrA*, *dsrB*, and *csyJ* were more abundant by 31% ($p = 0.01$), 35% ($p = 0.01$), and 40% ($p = 0.002$), respectively, in C1S1 as compared with

C0S0 under long-term submergence (Figure 5a), indicating their major role in dissimilatory sulfate reduction. Similarly, among C-cycling functional genes, phenol oxidase, and endochitinase were the most dominant genes and were 35% ($\rho = 0.002$) and 30% ($\rho = 0.017$) more abundant, respectively, in C1S1 than in C0S0 (Figure 5b). Metal resistance genes for Cd, Zn, and Pb were examined, and *cadA* (Cd resistance gene), *czcA* (Cd, Zn, and Co resistance gene), and *pbrA* (Pb resistant gene) decreased by 29% ($\rho = < 0.001$), 24% ($\rho = 0.002$), and 15% ($\rho = 0.002$), respectively, in C1S1 as compared with C0S0 over time (Figure 5c).

Canonical correspondence analysis (CCA) was performed to examine the relationship between microbial community structure and geochemistry (Figure 6) to correlate environmental variables with the functional community structure and determine the most significant variable causing the change in community structure. Environmental variables, such as dissolved organic carbon (DOC), SO_4^{2-} , total S, and NO_3^- (Table 1) were used to perform CCA.

No composite samples were prepared for detailed wet chemistry analysis that was utilized to plot CCA, therefore only two points are plotted for CCA.

In CCA, environmental variables are represented as arrows starting at the origin and pointing outward. Our CCA results show that DOC and S are closer, with a small angle indicating that these variables are more strongly correlated with the microbial community. Dissolved organic carbon and NO_3^- had longer arrows with larger angles, indicating that these variables have a stronger influence on the microbial community but in a different manner. The SO_4^{2-} and total S vectors are in opposite directions, indicating that these factors are negatively correlated. This could be explained as the total difference between total sulfur and sulfate is sulfide, indicating that under high S concentrations, sulfide formation has been favored.

Table 1. Chemical data for the effluent samples collected after medium- (119-day) and long- (252-day) term submergence. The soil samples collected at these time points were used for microarray analysis.

Sample	($\mu\text{g/L}$)			pH	(mg/L)		
	Zn	Cd	Pb		DOC	Sulfate-S	Nitrate-N
C0S0 119-day	723 \pm 40.9	432 \pm 10.9	<DL	7.57 \pm 0.02	5 \pm 0.03	474 \pm 10.25	2.0 \pm 0.1
C0S0 252-day	517 \pm 30.9	28 \pm 0.9	<DL	8.41 \pm 0.03	62 \pm 2.6	571 \pm 5.64	2.0 \pm 0.2
C0S1 119-day	30 \pm 1.7	2 \pm 0.01	<DL	8.00 \pm 0.02	4 \pm 0.1	468 \pm 6.78	1.8 \pm 0.5
C0S1 252-day	<DL	1 \pm 0.006	36 \pm 1.6	6.39 \pm 0.005	65 \pm 0.8	¶	2.2 \pm 0.02
C1S0 119-day	<DL	1 \pm 0.001	<DL	8.18 \pm 0.012	5 \pm 0.02	503 \pm 7.34	1.9 \pm 0.01
C1S0 252-day	<DL	<DL	<DL	7.58 \pm 0.015	<DL	474 \pm 3.95	2.0 \pm 0.05
C1S1 119-day	<DL	1 \pm 0.004	<DL	7.40 \pm 0.01	4 \pm 0.1	437 \pm 10.02	1.8 \pm 0.04
C1S1 252-day	<DL	<DL	<DL	7.02 \pm 0.01	<DL	288 \pm 8.64	1.9 \pm 0.14

DL corresponds to detection limit. Detection limit of 0.6 for Cd, and 0.7 $\mu\text{g/L}$ for Pb was determined. ¶ indicates data not collected.

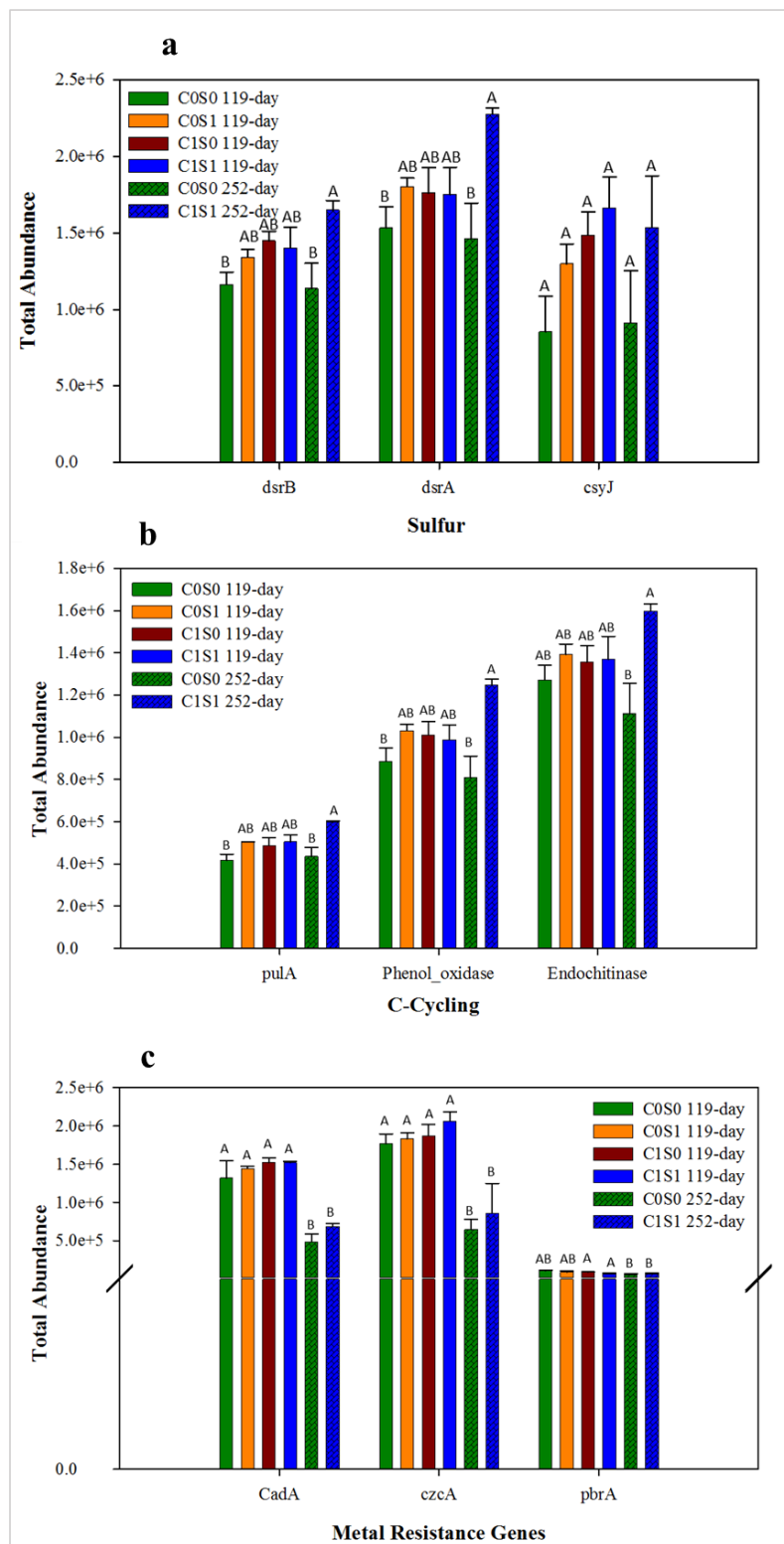


Figure 5. Total abundance of (a) *dsrA/dsrB*, and *csyJ* in the sulfur category; (b) *pula*, *Phenol_oxidase*, *Endochitinase* under the C-cycling category; and (c) Cd resistance gene (*CadA*), Zn resistance gene (*czcA*), and Pb resistance gene (*pbrA*). Vertical bars represent the mean of three replicates. All the treatments, COS0, COS1, C1S0, and C1S1 (solid filled bars), from medium-term submergence, and only COS0 and C1S1 (pattern filled bars) from long-term submergence are plotted. Vertical bars represent the mean of three replicates; two replicates from the individual columns and one replicate from the mixture of two columns. Bars with the same letter are not significantly different. Different letters within a category indicate significance difference ($\alpha = 0.05$).

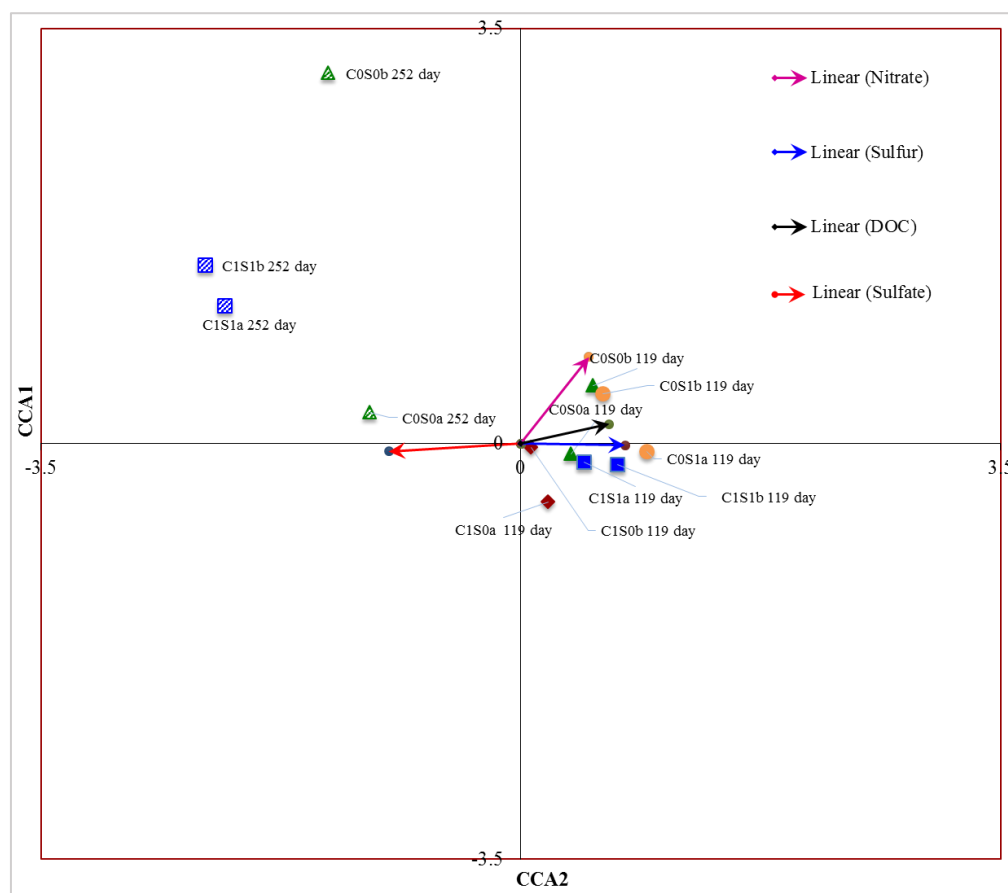


Figure 6. Canonical correspondence analysis (CCA) indicating the relationship between microbial communities with environmental factors.

4. Discussion

4.1. Preliminary Microbial Community Characterization

The contaminants effects on in situ microbiota are generally continuous and may trigger the loss or emergence of a genus or species of microorganism [44]. Higher abundance of Gram+, and fungi biomarkers were present in the starting materials as these communities are more successful in resource limited situations like mine impacted soils with fewer nutrients. On addition of inoculum followed by OC and S treatment, changes in PLFA composition and biomass were detected as compared to non-amended soil in medium-term submergence. This suggests that the OC and S additions in this study favored microbial growth pattern and composition resulting in change of microbial community structure. Specifically, branched monounsaturated cyclopropane PLFAs, characteristic of Gram+ bacteria, and cyclopropane PLFAs, characteristic of Gram- bacteria abundance, and branched fatty acid, i17:1, characteristic of *Desulfovibrio*, were increased on OC and S amendment, indicating that these PLFA biomarkers could be the main contributors in microbial community structure change in amended soil. The increased abundance of those microbial communities could be due to added OC and S, their prior presence, their capability to survive in adverse situations, and differences in substrate utilization [45,46]. Another reason could be due to increased metal resistance genes. Several Gram+ and Gram- soil bacteria that were isolated from Pb-contaminated sites have exhibited resistance to a range of metal ions, such as Pb, Zn, Cu, Cd, Co, and Hg [47]. The significant increase in *Desulfovibrio* biomarker could be result of dissimilatory sulfate reduction happening in the system due to OC and S addition.

4.2. Relationships among Microbial Communities

Detrended correspondence analysis conducted based on time indicated that there was not very clear clustering of microbial community based on OC and/or S treatments under medium-term submergence. Relatively more overlapping among the samples from C1S0, C0S1, and C0S0 systems were observed as compared to C1S1 (Figure S2), which suggests some closer association among the microorganisms from these treatments. The closely associated microbes could be due to common and flexible substrate utilization preference. Comparatively, lesser or no overlap was observed among the samples from C1S1 and C0S0 under longer submergence. The segregation among the clusters from these two treatments under different categories increased with time depending on their involvement in microbial community structure changes. This supports the fact that time was another dominant factor in determining the microbial community structure. The positive effect of OC, S, and N via increase in corresponding functional genes abundance and the impact on change in microbial community structure has been observed by several studies [48,49]. Overall, DCA results indicated that the decreases in metal resistance and organic remediation functional genes and enrichment in S- and C-cycling functional genes were mainly involved in the observed community shift.

4.3. Functional Gene Diversity

The significant increase in overall microbial community functional gene abundance in C1S1, followed by a significant decline (Figure 2) may indicate rapid oxidation of added OC coupled with a reduction in available terminal electron acceptors (TEAs) and a subsequent decline as suitable TEAs were exhausted. This result could be explained by the trend that was observed with DOC concentration in the current study. Initial concentration of DOC in the eluent was 32 mM but it was reduced to 30 mM in effluent at seven-day submergence and further decreased to below detection limit (DL) under long-term submergence in OC-added treatments. On the other hand, non-OC-treated columns showed <3 mM DOC, with no significant change during long-term submergence (Table 1). A similar result was reported by Brodie et al. [50], in which initial enrichment in total functional genes was observed with OC addition and subsequently declined, but no such enhancement in functional gene richness was observed without OC addition. Therefore, we speculate that these results could be owing to decreased availability of OC (<3 mM) (Table 1).

Previous studies revealed that the addition of OC stimulated biomass and microbial activity in these typically nutrient-poor environments and had a significant effect on microbial biomass, microbial community structure, and functional genes [51,52]. Sufficient labile OC must be available for sulfate reduction and it is a key rate-limiting factor in metal sulfide formation [52,53]. This process can be accelerated by the action of indigenous microorganisms fueled through the addition of exogenous carbon [54–56]. The change in microbial community structure was observed because of the direct or indirect response of certain functional genes, such as those involved in OC oxidation or TEA reduction or in altering environmental conditions. Similar observations were also reported in a study using GeoChip to examine the bioremediation of U (Van Nostrand et al. [55]). Several other studies that were conducted using other techniques, such as phospholipid fatty acid analysis (PLFA) and polymerase chain reactions-denaturing gradient gel electrophoresis (PCR-DGGE), reported changes in microbial community structure with the addition of OC as a substrate [56,57].

As previously mentioned, some of these genes represent background populations, whereas others may be directly involved in bio-reduction [58]. For example, if organic remediation genes are considered to represent background functional genes, their significant decrease (Figure 4b) is probably owing to an increase in genes that are directly involved in bio-reduction (i.e., *dsrA/B*) rather than a true reduction in organic remediation genes, because they are likely not involved in bio-reduction; a similar result was also reported by Van Nostrand et al. [55].

4.4. Total Abundance of Functional Gene Categories

The abundance of stress-related functional genes and metal resistance genes decreased during long-term submergence, with both C1S1 and C0S0 indicating that, in addition to OC and S, submergence time played a role in decreasing toxicity in these systems. Heavy metals are predicted to represent a major stress on the microbial community, and the adaptation to metal stress may be of importance in shaping microbial community structure [58]. Several studies have indicated the impact of heavy metals on microbial activities and their community structure [54,58]. A study conducted on the effects of Pb and Cd on soil microbial activities and their community structure via DGGE indicated that Pb and Cd together decreased the number of bacteria when no nutrients were supplied and revealed a significant impact on community structure dynamics, particularly at high Pb and Cd concentrations [54]. Increased activity of S-cycling functional genes could be owing to readily available sulfate as TEA under more reduced conditions, thereby favoring dissimilatory sulfate reduction, as reported before [50,59]. In the current study, the relationship observed between enhanced dissimilatory sulfate reduction and increased S-cycling functional genes can be further supported by the decreased sulfate-S concentration in effluent samples (Table 1) and the increased metal sulfide formation (Figure 1a–c). Direct involvement of C-cycling and S-cycling genes in dissimilatory S reduction via the rapid consumption of OC followed by sulfate reduction was also reported before by Huerta-Diaz et al. [60]. The changes in microbial communities result in changes in functional gene abundances.

Metal precipitation is one of the most significant processes involved in the long-term retention of metals in artificial and natural wetlands. Such processes may be accompanied by other indirect reductive metal precipitation (such as redox transformation), including dissimilatory sulfate reduction and the subsequent precipitation of metal sulfides [60]. As reported in Karna et al. [31], our results also suggest that appropriate microbial communities were stimulated by OC- and/or S- treatments and they resulted in rapid immobilization of Pb, Zn, and Cd in both C1S0 and C1S1 under medium- and long-term submergence. The reduction of metals concentration in solution were most likely due to biogeochemical transformations of Pb, Zn and Cd under reduced conditions. This was supported by bulk XAS results, indicating increasing galena (PbS), sphalerite (ZnS), and cadmium sulfide formations in C1S1 over time [31]. A similar amount of galena formation was also observed in C1S0. Limited S concentration and enhanced pH in C1S0 treatment, however, could lead metal carbonates to be more dominant in the long run and control metal solubility. Metal carbonates are more vulnerable to changing environmental conditions, whereas metal sulfides can be resistant to reoxidation. Therefore, treatment with both OC and S would be a more promising strategy to maintain permissibly low metal concentrations in water for a longer period.

A handful of studies have examined non-redox-sensitive element removal via constructed wetland treatment systems [3,40]. Earlier studies by Almendras et al. [6] tested Pb, Cu, and Zn stability via sulfide formations and showed that biostimulation plays a vital role in stabilizing Pb, Zn and Cd in the subsurface environment. The results from our study also suggest that wetland construction can be a better alternative for stabilizing non-redox-sensitive elements, such as Pb, Zn, and Cd in mine waste materials or similar geomaterial. The uniqueness of this study is that the microbial analyses that are presented here in detail are in agreement with molecular-scale synchrotron-based X-ray data [31]. Combining advanced microbiological techniques with synchrotron-based speciation enhances our understanding of the biogeochemical processes that are involved in Pb and Zn removal via dissimilatory sulfate reductions under reduced conditions. The results obtained from the current study indicate that OC and S addition stimulated microbial growth and activities, causing changes in the functional microbial community structure via the enhancement or reduction of functional genes in saturated mine waste materials enriched with Pb and Zn. The decrease in metal resistance genes indicated reduced toxicity over time. Correspondingly, enrichment in S- and C-cycling genes in OC- and/or S-treated samples corroborated that these members made significant contributions to the metal stability in the highly contaminated mine waste in a subsurface environment. Sulfate-reducing bacteria

gene *dsrA/B* appeared to be a key player in forming metal sulfides and was significantly enhanced in C1S1 during long-term submergence. On the other hand, no significant difference was detected in functional gene richness in any C0S0 treatment category over time. The information obtained from this study help us conclude that biostimulation would be beneficial for inducing metal sulfide formations in mine waste materials and that SRB can be used as key players in in situ bioremediation of Pb and Zn in subsurface treatment wetlands.

Supplementary Materials: The following are available online at <http://www.mdpi.com/2571-8789/2/4/60/s1>. Figure S1: Detrended correspondence analysis (DCA) for the total number of detected genes under medium- (119-day) and long-term (252-day) submergence indicating community structure changes. All the treatments; C0S0, C0S1, C1S0, and C1S1 (solid filled markers) from medium-term submergence, and only C0S0, and C1S1 (pattern filled markers) from long-term submergence are plotted; Figure S2: Detrended correspondence analysis (DCA) of functional genes in the metal resistance category showing change in community structure under medium- (119-day) and long-term (252-day) submergence. All the treatments; C0S0, C0S1, C1S0, and C1S1 (solid filled markers) from medium-term submergence, and only C0S0, and C1S1 (pattern filled markers) from long-term submergence are plotted; Figure S3: Detrended correspondence analysis (DCA) of functional genes in the C-cycling category showing change in community structure under medium- (119-day) and long-term (252-day) submergence. All the treatments; C0S0, C0S1, C1S0, and C1S1 (solid filled markers) from medium-term submergence, and only C0S0, and C1S1 (pattern filled markers) from long-term submergence are plotted; Figure S4: Detrended correspondence analysis (DCA) of functional genes in the sulfur category showing change in community structure under medium- (119-day), and long-term (252-day) submergence. All the treatments; C0S0, C0S1, C1S0, and C1S1 (solid filled markers) from medium-term submergence, and only C0S0, and C1S1 (pattern filled markers) from long-term submergence are plotted; Figure S5: Detrended correspondence analysis (DCA) of *dsrB* showing a change in community structure under medium- (119-day), and long-term (252-day) submergence. All the treatments; C0S0, C0S1, C1S0, and C1S1 (solid filled markers) from medium-term submergence, and only C0S0, and C1S1 (pattern filled markers) from long-term submergence are plotted; Figure S6: Detrended correspondence analysis (statistics) of *dsrA* showing a change in community structure under medium- (119-day), and long-term (252-day) submergence. All the treatments; C0S0, C0S1, C1S0, and C1S1 (solid filled markers) from medium-term submergence, and only C0S0, and C1S1 (pattern filled markers) from long-term submergence are plotted; Table S1: Total element concentration in the mine waste fraction of <2mm collected from the Tri-State mining district; Table S2: Summary of total phospholipid fatty acid analysis (PLFA) biomarkers detected in original mine tailings, submerged control, and submerged treated materials under 119-day (medium-term) submergence; Table S3: Bray Curtis dissimilarity test giving ρ -value for each treatment during medium- (119-day) and long-term (252-day) submergence.

Author Contributions: R.K. and G.M.H. conceived and designed the study, R.K. performed the experiments with the support of G.M.H., and wrote the paper with input from G.M.H. and J.V.N., T.Y. assisted in collecting the microarray data at the institute of Environmental Genomics. J.V.N., C.W.R. and J.Z. assisted in data analysis and data interpretation. Y.A. assisted in statistical analysis. All the authors reviewed and contributed to the final version of the manuscript.

Funding: This research was funded by the Kansas Agricultural Experimental Station, and the USDA National Institute of Food and Agriculture Multistate Research Project grant number [NC-1187].

Acknowledgments: We thank Gary M. Pierzynski, Gerard Kluitenberg, and Saugata Datta, for their helpful suggestions and insightful discussions. We also acknowledge Ye Deng for his help with microarray data collection and inputs for analysis. We thank Ari Jumponen and his students for providing lab space to conduct initial procedure in DNA extraction and purification procedures. We are thankful to Dorothy Menefee for her help during experimental set up, and Pavithra P. Arachchige for help during data collection. We would also like to acknowledge Kansas Agric. Exp. Stn (Contribution # 15-212-J) and Derek Peloquin for proof reading the manuscript.

Conflicts of Interest: The authors declare no conflict of interest.

References

1. Adriano, D.C. *Trace Elements in Terrestrial Environments: Biogeochemistry, Bioavailability, and Risks of Metals*; Springer: New York, NY, USA, 2001.
2. Bhattacharya, J.; Ji, S.W.; Lee, H.S.; Cheong, Y.W.; Yim, G.J.; Min, J.S.; Choi, Y.S. Treatment of acidic coal mine drainage: Design and operational challenges of successive alkalinity producing systems. *Mine Water Environ.* **2008**, *27*, 12–19. [[CrossRef](#)]
3. Almendras, M.; Wiertz, J.V.; Chamy, R. Heavy metals immobilization in contaminated smelter soils using microbial sulphate reduction. In *Advanced Materials Research*; Trans Tech Publications: Princeton, NJ, USA, 2009; Volume 71, pp. 577–580.

4. Johnson, D.B.; Hallberg, K.B. Acid mine drainage remediation options: A review. *Sci. Total Environ.* **2005**, *338*, 3–14. [[CrossRef](#)] [[PubMed](#)]
5. Pierzynski, G.M.; Vaillant, G.C. Remediation to reduce ecological risk from trace element contamination: A decision case study. *Collect. Case Stud.* **2018**, 9–18. Available online: <https://dl.sciencesocieties.org/publications/books/abstracts/acesspublicati/casestudies/9?access=0&view=pdf>. (accessed on 3 November 2018).
6. Hayes, J.M.; Waldbauer, J.R. The carbon cycle and associated redox processes through time. *Philos. Trans. R. Soc. Lond. B* **2006**, *361*, 931–950. [[CrossRef](#)] [[PubMed](#)]
7. Stein, O.R.; Borden-Stewart, D.J.; Hook, P.B.; Jones, W.L. Seasonal influence on sulfate reduction and zinc sequestration in subsurface treatment wetlands. *Water Res.* **2007**, *41*, 3440–3448. [[CrossRef](#)] [[PubMed](#)]
8. Zhang, S.H.; Xue, X.X.; Liu, R.; Jin, Z.F. Current Situation and Prospect of the Comprehensive Utilization of mining tailings. *Min. Metall. Eng.* **2005**, *3*, 44–48.
9. Borch, T.; Kretzschmar, R.; Kappler, A.; Cappellen, P.V.; Ginder-Vogel, M.; Voegelin, A.; Campbell, K. Biogeochemical redox processes and their impact on contaminant dynamics. *Environ. Sci. Technol.* **2009**, *44*, 15–23. [[CrossRef](#)] [[PubMed](#)]
10. Evans, M.; Warburton, J.; Yang, J. Eroding blanket peat catchments: Global and local implications of upland organic sediment budgets. *Geomorphology* **2006**, *79*, 45–57. [[CrossRef](#)]
11. Toevs, G.R.; Morra, M.J.; Polizzotto, M.L.; Strawn, D.G.; Bostick, B.C.; Fendorf, S. Metal (loid) diagenesis in mine-impacted sediments of Lake Coeur d’Alene, Idaho. *Environ. Sci. Technol.* **2006**, *40*, 2537–2543. [[CrossRef](#)] [[PubMed](#)]
12. Burton, E.D.; Bush, R.T.; Sullivan, L.A.; Mitchell, D.R. Schwertmannite transformation to goethite via the Fe (II) pathway: Reaction rates and implications for iron–sulfide formation. *Geochim. Cosmochim. Acta* **2008**, *72*, 4551–4564. [[CrossRef](#)]
13. Chen, X.; Wright, J.V.; Conca, J.L.; Peurrung, L.M. Effects of pH on heavy metal sorption on mineral apatite. *Environ. Sci. Technol.* **1997**, *31*, 624–631. [[CrossRef](#)]
14. MacLean, L.C.W.; Pray, T.J.; Onstott, T.C.; Brodie, E.L.; Hazen, T.C.; Southam, G. Mineralogical, chemical and biological characterization of an anaerobic biofilm collected from a borehole in a deep gold mine in South Africa. *Geomicrobiol. J.* **2007**, *24*, 491–504. [[CrossRef](#)]
15. Bazyliński, D.A.; Frankel, R.B. Biologically controlled mineralization in prokaryotes. *Rev. Mineral. Geochem.* **2003**, *54*, 217–247. [[CrossRef](#)]
16. Whiteman, M.; Armstrong, J.S.; Chu, S.H.; Jia-Ling, S.; Wong, B.S.; Cheung, N.S.; Halliwell, B.; Moore, P.K. The novel neuromodulator hydrogen sulfide: An endogenous peroxyxynitrite ‘scavenger’? *J. Neurochem.* **2004**, *90*, 765–768. [[CrossRef](#)] [[PubMed](#)]
17. He, Z.; Gentry, T.J.; Schadt, C.W.; Wu, L.; Liebich, J.; Chong, S.C.; Huang, Z.; Wu, W.; Gu, B.; Jardine, P.; et al. GeoChip: A comprehensive microarray for investigating biogeochemical, ecological and environmental processes. *ISME J.* **2007**, *1*, 67. [[CrossRef](#)] [[PubMed](#)]
18. Van Nostrand, J.D.; Wu, W.M.; Wu, L.; Deng, Y.; Carley, J.; Carroll, S.; He, Z.; Gu, B.; Luo, J.; Criddle, C.S.; et al. GeoChip-based analysis of functional microbial communities during the reoxidation of a bioreduced uranium-contaminated aquifer. *Environ. Microbiol.* **2009**, *11*, 2611–2626. [[CrossRef](#)] [[PubMed](#)]
19. Tu, Q.; Yu, H.; He, Z.; Deng, Y.; Wu, L.; Van Nostrand, J.D.; Zhou, A.; Voordeckers, J.; Lee, Y.J.; Qin, Y.; et al. GeoChip 4: A functional gene-array-based high-throughput environmental technology for microbial community analysis. *Mol. Ecol. Resour.* **2014**, *14*, 914–928. [[CrossRef](#)] [[PubMed](#)]
20. Loick, N.; Weisener, C. Novel molecular tools to assess microbial activity in contaminated environments. In *Geomicrobiology and Biogeochemistry*; Springer: Berlin/Heidelberg, Germany, 2014; pp. 17–35.
21. Lu, Z.; Deng, Y.; Van Nostrand, J.D.; He, Z.; Voordeckers, J.; Zhou, A.; Lee, Y.J.; Mason, O.U.; Dubinsky, E.A.; Chavarria, K.L.; et al. Microbial gene functions enriched in the Deepwater Horizon deep-sea oil plume. *ISME J.* **2012**, *6*, 451. [[CrossRef](#)] [[PubMed](#)]
22. Frostegård, Å.; Tunlid, A.; Bååth, E. Use and misuse of PLFA measurements in soils. *Soil Biol. Biochem.* **2011**, *43*, 1621–1625. [[CrossRef](#)]
23. Olsson, P.A. Signature fatty acids provide tools for determination of the distribution and interactions of mycorrhizal fungi in soil. *FEMS Microbiol. Ecol.* **1999**, *29*, 303–310. [[CrossRef](#)]
24. Brantley, S.L.; Goldhaber, M.B.; Ragnarsdottir, K.V. Crossing disciplines and scales to understand the critical zone. *Elements* **2007**, *3*, 307–314. [[CrossRef](#)]

25. Brown, G.E.; Foster, A.L.; Ostergren, J.D. Mineral surfaces and bioavailability of heavy metals: A molecular-scale perspective. *Proc. Natl. Acad. Sci. USA* **1999**, *96*, 3388–3395. [[CrossRef](#)] [[PubMed](#)]
26. Kilmer, V.J.; Alexander, L.T. Methods of making mechanical analyses of soils. *Soil Sci.* **1949**, *68*, 15–24. [[CrossRef](#)]
27. Soil Survey Laboratory Staff. *Soil Survey Laboratory Manual. Soil Survey Investigation*; Report No. 42 USDA-NRCS; U.S. Government Printing Office: Washington, DC, USA, 1996.
28. Zarcinas, B.A.; McLaughlin, M.J.; Smart, M.K. The effect of acid digestion technique on the performance of nebulization systems used in inductively coupled plasma spectrometry. *Commun. Soil Sci. Plant Anal.* **1996**, *27*, 1331–1354. [[CrossRef](#)]
29. Luptakova, A.; Kusnierova, M. Bioremediation of acid mine drainage contaminated by SRB. *Hydrometallurgy* **2005**, *77*, 97–102. [[CrossRef](#)]
30. Wan, J.; Tokunaga, T.K.; Brodie, E.; Wang, Z.; Zheng, Z.; Herman, D.; Hazen, T.C.; Firestone, M.K.; Sutton, S.R. Reoxidation of bioreduced uranium under reducing conditions. *Environ. Sci. Technol.* **2005**, *39*, 6162–6169. [[CrossRef](#)] [[PubMed](#)]
31. Karna, R.R.; Hettiarachchi, G.M.; Newville, M.; Sun, C.; Ma, Q. Synchrotron-based X-ray spectroscopy studies for redox-based remediation of lead, zinc, and cadmium in mine waste materials. *J. Environ. Qual.* **2016**, *45*, 1883–1893. [[CrossRef](#)] [[PubMed](#)]
32. Bligh, E.G.; Dyer, W.J. A rapid method of total lipid extraction and purification. *Can. J. Biochem. Physiol.* **1959**, *37*, 911–917. [[CrossRef](#)] [[PubMed](#)]
33. White, D.C.; Ringelberg, D.B. Signature lipid biomarker analysis. *Tech. Microb. Ecol.* **1998**, *1*, 255–272.
34. McKinley, V.L.; Peacock, A.D.; White, D.C. Microbial community PLFA and PHB responses to ecosystem restoration in tallgrass prairie soils. *Soil Biol. Biochem.* **2005**, *37*, 1946–1958. [[CrossRef](#)]
35. Liang, Y.; Van Nostrand, J.D.; Deng, Y.; He, Z.; Wu, L.; Zhang, X.; Li, G.; Zhou, J. Functional gene diversity of soil microbial communities from five oil-contaminated fields in China. *ISME J.* **2011**, *5*, 403. [[CrossRef](#)] [[PubMed](#)]
36. Heald, S.M.; Cross, J.O.; Brewster, D.L.; Gordon, R.A. Nuclear instruments and methods in physics research section A: Accelerators, spectrometers, detectors and associated equipment. *Proc. Natl. Conf. Synchrotron Radiat. Res.* **2007**, *582*, 215–217.
37. Manceau, A.; Marcus, M.A.; Tamura, N. Quantitative speciation of heavy metals in soils and sediments by synchrotron X-ray techniques. *Rev. Mineral. Geochem.* **2002**, *49*, 341–428. [[CrossRef](#)]
38. Scheinost, A.C.; Kretzschmar, R.; Pfister, S.; Roberts, D.R. Combining selective sequential extractions, X-ray absorption spectroscopy, and principal component analysis for quantitative zinc speciation in soil. *Environ. Sci. Technol.* **2002**, *36*, 5021–5028. [[CrossRef](#)] [[PubMed](#)]
39. Roberts, D.R.; Scheinost, A.; Sparks, D. Zinc speciation in a smelter contaminated soil profile using bulk and microspectroscopic techniques. *Environ. Sci. Technol.* **2002**, *36*, 1742–1750. [[CrossRef](#)] [[PubMed](#)]
40. White, C.; Gadd, G.M. Copper accumulation by sulfate-reducing bacterial biofilms. *FEMS Microbiol. Lett.* **2000**, *183*, 313–318. [[CrossRef](#)] [[PubMed](#)]
41. Janssen, G.M.; Temminghoff, E.J. In situ metal precipitation in a zinc-contaminated, aerobic sandy aquifer by means of biological sulfate reduction. *Environ. Sci. Technol.* **2004**, *38*, 4002–4011. [[CrossRef](#)] [[PubMed](#)]
42. Kirk, M.F.; Holm, T.R.; Park, J.; Jin, Q.; Sanford, R.A.; Fouke, B.W.; Bethke, C.M. Bacterial sulfate reduction limits natural arsenic contamination in groundwater. *Geology* **2004**, *32*, 953–956. [[CrossRef](#)]
43. Klein, M.; Friedrich, M.; Roger, A.J.; Hugenholtz, P.; Fishbain, S.; Abicht, H.; Blackall, L.L.; Stahl, D.A.; Wagner, M. Multiple lateral transfers of dissimilatory sulfite reductase genes between major lineages of sulfate-reducing prokaryotes. *J. Bacteriol.* **2001**, *183*, 6028–6035. [[CrossRef](#)] [[PubMed](#)]
44. Smith, G.A.; Nickels, J.S.; Kerger, B.D.; Davis, J.D.; Collins, S.P.; Wilson, J.T.; McNabb, J.F.; White, D.C. Quantitative characterization of microbial biomass and community structure in subsurface material: A prokaryotic consortium responsive to organic contamination. *Can. J. Microbiol.* **1986**, *32*, 104–111. [[CrossRef](#)]
45. Bossio, D.A.; Scow, K.M. Impacts of carbon and flooding on soil microbial communities: Phospholipid fatty acid profiles and substrate utilization patterns. *Microb. Ecol.* **1998**, *35*, 265–278. [[CrossRef](#)] [[PubMed](#)]
46. Ibekwe, A.M.; Kennedy, A.C. Phospholipid fatty acid profiles and carbon utilization patterns for analysis of microbial community structure under field and greenhouse conditions. *FEMS Microbiol. Ecol.* **1998**, *26*, 151–163. [[CrossRef](#)]

47. Trajanovska, S.; Britz, M.L.; Bhawe, M. Detection of heavy metal ion resistance genes in Gram-positive and Gram-negative bacteria isolated from a lead-contaminated site. *Biodegradation* **1997**, *8*, 113–124. [[CrossRef](#)] [[PubMed](#)]
48. Fuhrman, J.A. Microbial community structure and its functional implications. *Nature* **2009**, *459*, 193–199. [[CrossRef](#)] [[PubMed](#)]
49. Tokunaga, T.K.; Wan, J.; Firestone, M.K.; Hazen, T.C.; Olson, K.R.; Herman, D.J.; Sutton, S.R.; Lanzirrotti, A. In situ reduction of chromium (VI) in heavily contaminated soils through organic carbon amendment. *J. Environ. Qual.* **2003**, *32*, 1641–1649. [[CrossRef](#)] [[PubMed](#)]
50. Brodie, E.L.; DeSantis, T.Z.; Joyner, D.C.; Baek, S.M.; Larsen, J.T.; Andersen, G.L.; Hazen, T.C.; Richardson, P.M.; Herman, D.J.; Tokunaga, T.K.; et al. Application of a high-density oligonucleotide microarray approach to study bacterial population dynamics during uranium reduction and reoxidation. *Appl. Environ. Microbiol.* **2006**, *72*, 6288–6298. [[CrossRef](#)] [[PubMed](#)]
51. Yergeau, E.; Kang, S.; He, Z.; Zhou, J.; Kowalchuk, G.A. Functional microarray analysis of nitrogen and carbon cycling genes across an Antarctic latitudinal transect. *ISME J.* **2007**, *1*, 163. [[CrossRef](#)] [[PubMed](#)]
52. Ku, T.C.; Kay, J.; Browne, E.; Martini, A.M.; Peters, S.C.; Chen, M.D. Pyritization of iron in tropical coastal sediments: Implications for the development of iron, sulfur, and carbon diagenetic properties, Saint Lucia, Lesser Antilles. *Mar. Geol.* **2008**, *249*, 184–205. [[CrossRef](#)]
53. Morse, J.W.; Luther, G.W., III. Chemical influences on trace metal-sulfide interactions in anoxic sediments. *Geochim. Cosmochim. Acta* **1999**, *63*, 3373–3378. [[CrossRef](#)]
54. Khan, S.; Hesham, A.E.L.; Qiao, M.; Rehman, S.; He, J.Z. Effects of Cd and Pb on soil microbial community structure and activities. *Environ. Sci. Pollut. Res.* **2010**, *17*, 288–296. [[CrossRef](#)] [[PubMed](#)]
55. Van Nostrand, J.D.; Wu, L.; Wu, W.M.; Huang, Z.; Gentry, T.J.; Deng, Y.; Carley, J.; Carroll, S.; He, Z.; Gu, B.; et al. Dynamics of microbial community composition and function during in-situ bioremediation of a uranium-contaminated aquifer. *Appl. Environ. Microbiol.* **2011**. [[CrossRef](#)] [[PubMed](#)]
56. Calbrix, R.; Barray, S.; Chabrierie, O.; Fourrie, L.; Laval, K. Impact of organic amendments on the dynamics of soil microbial biomass and bacterial communities in cultivated land. *Appl. Soil Ecol.* **2007**, *35*, 511–522. [[CrossRef](#)]
57. Eiler, A.; Langenheder, S.; Bertilsson, S.; Tranvik, L.J. Heterotrophic bacterial growth efficiency and community structure at different natural organic carbon concentrations. *Appl. Environ. Microbiol.* **2003**, *69*, 3701–3709. [[CrossRef](#)] [[PubMed](#)]
58. Hemme, C.L.; Deng, Y.; Gentry, T.J.; Fields, M.W.; Wu, L.; Barua, S.; Barry, K.; Tringe, S.G.; Watson, D.B.; He, Z.; et al. Metagenomic insights into evolution of a heavy metal-contaminated groundwater microbial community. *ISME J.* **2010**, *4*, 660. [[CrossRef](#)] [[PubMed](#)]
59. Muyzer, G.; Stams, A.J. The ecology and biotechnology of sulphate-reducing bacteria. *Nat. Rev. Microbiol.* **2008**, *6*, 441. [[CrossRef](#)] [[PubMed](#)]
60. Huerta-Diaz, M.A.; Tessier, A.; Carignan, R. Geochemistry of trace metals associated with reduced sulfur in freshwater sediments. *Appl. Geochem.* **1998**, *13*, 213–233. [[CrossRef](#)]

